

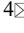





Integrated geophysical and aerial photogrammetry approach for detailed delineation of iron ore mineralization in lateritic deposits

Muhammad Junaid^{1,2}, Furqan Khan³, Badee Alshameri⁴,
Sami Ullah Shah⁵, Muhammad Zaka Emad^{6*}, Tariq Feroze²

¹ GEOTECH 2.0 Research Lab, Engineering College, Prince Sultan University, Riyadh, Saudi Arabia

² Department of Sustainable Advanced Geomechanical Engineering, National University of Sciences and Technology, Risalpur, Pakistan

³ Department of Mining Engineering, Karakoram International University, Gilgit-Baltistan, Pakistan

⁴ Department of Geotechnical Engineering, National University of Sciences and Technology, Islamabad, Pakistan

⁵ Department of Construction Engineering and Management and Surveying, National University of Sciences and Technology, Risalpur, Pakistan

⁶ College of Petroleum Engineering & Geosciences, King Fahd University of Petroleum & Minerals, Dhahran, Saudi Arabia

*Corresponding author: e-mail muhammadzaka.emad@kfupm.edu.sa

Abstract

Purpose. This study integrates unmanned aerial vehicles (UAVs) and Magnetic and 2D Electrical Resistivity Tomography (2D ERT) surveys to delineate subsurface laterite ore mineralization zones while reducing exploration costs. UAV imagery enabled the reconstruction of high-resolution digital elevation models and orthomosaics, providing detailed topographic information for survey planning.

Methods. Magnetic survey integrated with 2D electrical resistivity tomography (ERT) profiles were applied to characterize subsurface lithology and identify layers such as topsoil, shale, and laterite.

Findings. The ERT survey reveals that the topsoil is 3 meters thick and has a resistivity range of 10-50 Ω .m. The resistivity of shale varied between 50 and 150 Ω .m, with a thickness of two meters. The laterite ore was identified with resistivity values between 150 and 1200 Ω .m and a thickness of 5 m. Magnetic surveys identified magnetic anomalies of 200-600 nT, estimated at a depth of 3-5 m using forward modeling. Regional-scale interpretations from total magnetic intensity (TMI), reduced-to-pole (RTP), and continuation maps highlighted the detailed distribution of the magnetic anomalies throughout the study area, lithological variations, fault systems, and deep-seated magnetized bodies.

Originality. This study demonstrates an integrated, low-cost workflow for lateritic mineralization that uses detailed geophysical data, including magnetic methods, 2D ERT, and UAV photogrammetry. Conventional techniques are quite expensive relative to the value of the ore.

Practical implications. The results demonstrate that the integration of aerial photogrammetry, magnetic surveys, and 2D electrical resistivity tomography provides an efficient and cost-effective approach for delineating laterite ore mineralization zones and can serve as a viable alternative to conventional exploration methods.

Keywords: laterite ore; electrical resistivity tomography; magnetic survey; unmanned aerial vehicle; mineral exploration

1. Introduction

Laterites form as residual products of rock weathering [1]. Laterite ore deposits represent a significant geological resource with diverse industrial applications [2]. These deposits primarily consist of iron, bauxite, and other valuable metals, making them crucial as key ingredients in cement production [3], [4]. Rapid industrialization and population growth accelerated the development of new infrastructure, including megastructures and housing societies. Consequently, the demand for cement has surged, leading to a corresponding increase in the demand for laterite [5], [6].

Mineral exploration and resource characterization using integrated geophysical and remote-sensing methods have

advanced significantly over the last few years [7], [8]. Classic exploration for laterite and iron ore deposits has traditionally been based on extensive geological mapping, geochemical sampling, and drilling campaigns that are accurate but often cost-prohibitive and spatially limited [9], [10]. New avenues for quick, high-resolution mapping of both underground and surface facilities are available owing to lightweight geophysical equipment and UAVs [11].

Electrical Resistivity Tomography has proven particularly effective in lateritic environments, as it is sensitive not only to variations in lithology but also to moisture content, allowing the delineation of weathering profiles and distinguishing conductive, clay-rich overburden from more resis-

Received: 9 December 2025. Accepted: 6 March 2026. Available online: 30 March 2026

© 2026. M. Junaid et al.

Mining of Mineral Deposits. ISSN 2415-3443 (Online) | ISSN 2415-3435 (Print)

This is an Open Access article distributed under the terms of the Creative Commons Attribution License (<http://creativecommons.org/licenses/by/4.0/>), which permits unrestricted reuse, distribution, and reproduction in any medium, provided the original work is properly cited.

tive lateritic duricrust and bedrock [12]. Several studies in analogous tropical and subtropical terrains, such as in Brazil and West Africa, have successfully used 2D ERT to map the thickness of laterite caps and infer the geometry of the weathering front, providing critical data for reserve estimation. Magnetic surveys are a cornerstone of iron ore exploration, given the high magnetic susceptibility of magnetite and maghemite, which are commonly associated with these deposits. Aeromagnetic and ground magnetic data are usually employed to identify structural controls, map lithological contacts, and estimate the depth to magnetic sources, enabling regional to local targeting.

The emergence of Unmanned Aerial Vehicles has revolutionized the initial phases of site characterization. UAV-based photogrammetry provides centimeter-resolution digital elevation models and orthomosaics at a fraction of the cost and time of traditional topographic surveys or manned airborne LiDAR. High-resolution topographic data is not only crucial for the accurate design of geophysical surveys and topographic correction but also for geomorphological analysis, which can indicate near-surface geological structure [13]. The integration of complex data is a major strength of newer exploration techniques. However, data integration is where the true power of modern exploration lies. Synthesizing topographic, resistivity, and magnetic datasets within a GIS framework enables synergistic interpretation that reduces the ambiguity inherent in any single method. For example, a magnetic anomaly may be corroborated by a corresponding resistivity contrast and placed within an accurate topographic context to yield more robust geological modelling [14]. However, a significant research gap exists regarding the systematic application of this integrated UAV-geophysical methodology to the specific context of Pakistani laterite deposits, particularly those in Khyber Pakhtunkhwa. While regional geological studies have cataloged these resources [15], there is a paucity of published work employing modern multi-parameter geophysical techniques for their detailed, deposit-scale characterization. The present study focuses on bridging this gap. It aims to develop a tailored, cost-efficient exploration framework that combines UAV photogrammetry, 2D ERT, and ground magnetic surveys to model a laterite deposit at Nizampur with accuracy, thereby providing a useful case study for the evolving literature on technology-driven mineral exploration.

In the same scenario, Pakistan also experiences a surge in demand for laterite ore. Currently, 24 cement plants operate in Pakistan, with an average production of 5000 tons/day [16]. Based on the requirement for approximately 2% laterite in the cement raw mix, this corresponds to an estimated daily consumption of about 2400 tons. With the recent issuance of licenses for cement plants, demand for laterite ore is expected to grow in Pakistan in the coming years.

Laterite ore is widely distributed across Pakistan, especially in Baluchistan, Sindh, Punjab, and Khyber Pakhtunkhwa. In Khyber Pakhtunkhwa, laterite ore deposits are found in different districts, including D.I. Khan, Chitral, North Waziristan, Malakand, and Nowshera [15], [17]. Notably, the Nizampur iron deposits at the base of the Datta formation are estimated at 100 million tonnes of sedimentary hematite (25-35% Fe).

Given the economic significance of laterite ores, the utilization of efficient exploration techniques is crucial for dis-

covering viable deposits [9]. Traditional methods often entail costly, time-consuming processes, resulting in inefficient resource utilization [10], [18], [19]. However, advancements in multi-source data integration offer innovative solutions for rapid, cost-effective exploration [20]. The estimated iron ore resources in Khyber Pakhtunkhwa are estimated to exceed 200 million tonnes with an average of 30% Fe (in-situ grade), primarily in sedimentary blocks in the southern parts of the province. Major laterite deposits are found in areas such as Pezu (District Lakki Marwat), Smana (District Hangu), Nizampur (District Nowshera), and lower Hazara (District Haripur & Abbottabad) [21]. These deposits justify systematic development targeting the cement industries.

This research aims to explore laterite ore deposits using a multi-source data approach, integrating data from Unmanned Aerial Vehicle (UAV), 2D Electrical Resistivity Tomography (2D ERT), field measurements, and magnetic surveys. The primary objective of the study was to determine the thicknesses of the overburden and iron ore with precision and to identify the distribution of magnetic anomalies throughout the study area. For this purpose, a UAV survey was conducted to obtain precise topographic information for planning ERT and magnetic profiles. The 2D ERT, combined with a field survey, accurately determines the thicknesses of the overburden and iron ore. At the same time, the magnetic survey enables us to identify magnetic anomalies in the study area and estimate their depths using forward modelling. The interpretation of magnetic data in the form of Total Magnetic Intensity (TMI), Reduced to Pole (RTP), and a continuation map comprehensively determines the distribution of magnetic anomalies in the study area.

2. Study area

2.1. Geotectonic setting

Iron ore is generally metasomatic, magmatic, hydrothermal, sedimentary, or residual. The sedimentary iron deposit is most important because it provides around 80% of the world's iron ore. Pakistan also has many sedimentary iron ore deposits across various parts of the country, including Kalabagh, Langrial, Dilband, and Nizampur. The study area is in Nizampur, Nowshera, Pakistan, and lies on the Mesozoic shelf carbonate sequence shown in Figure 1a.

The above-mentioned sequence belongs to Kala Chitta Range. The rock belonging to the Kala Chitta Range transitioned between meta-sediments of the Lesser Himalayas to the north and the foreland basin to the south. The iron ore deposit of the Nizampur area lies towards the north of the Kala Chitta Range in the vicinity of the tectonic contact with the Attock Cherat Range. These ranges are located in the western foothills of the Great Himalaya. The age of these sedimentary rock sequences ranges from Permian to Quaternary [22]. The study area is above 240 m, as depicted in Figure 1b, c.

2.2. Geology

The main rock formation exposed in the form of an iron-bearing area belongs to the Kingriali Formation (late Triassic), which is overlain uncomfortably by the Datta Formation (Early Jurassic) and the Samana Suk Formation (Middle Jurassic) – consolidated gravel, silt and clays of quaternary age uncomfortably overlay all the mentioned formations.

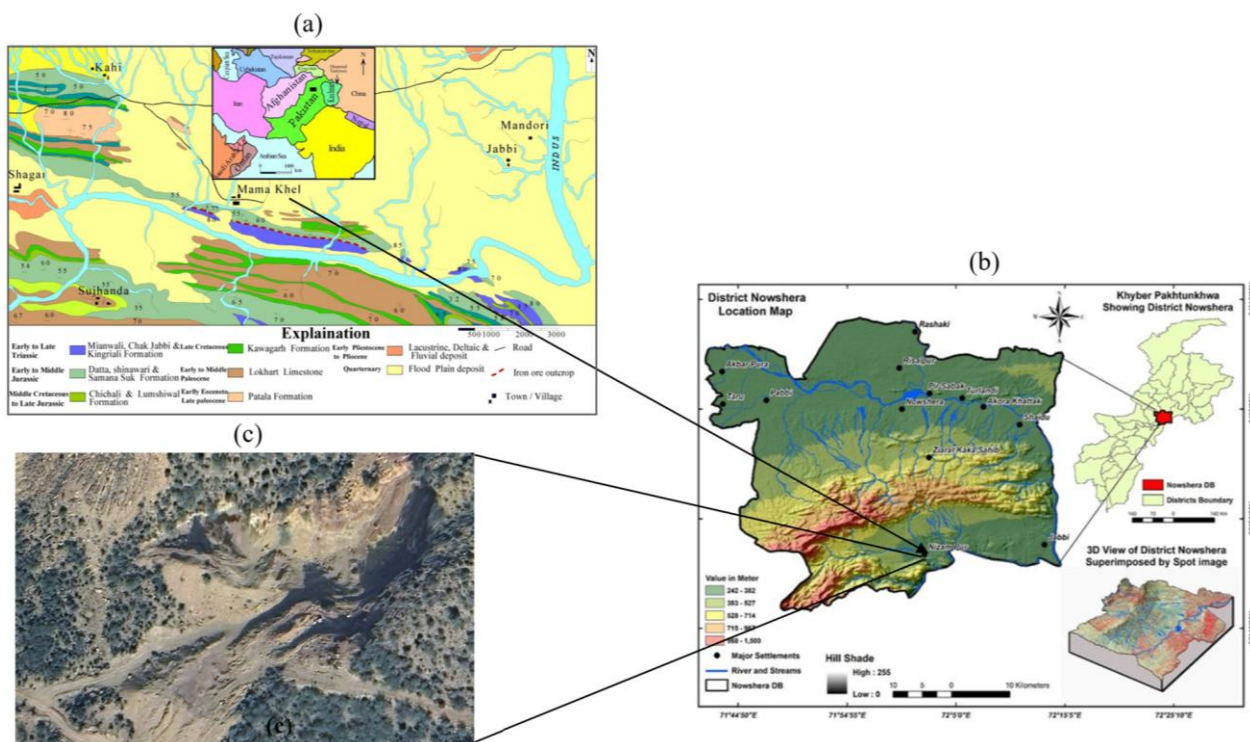


Figure 1. Geological map of the Study area: (a) geological map of Nowshera, Pakistan; (b) elevation map of Nowshera; (c) study area [23], [24]

The Kingriali formation is mostly composed of light greyish brown to yellow, ranging from thin to thick beds, and massive dolomite and dolomitic limestone – the dolomite grades upwards into yellowish green shale and marl. The overall formation thickness in the study area is approximately 90 metres. The lower contact with the Middle Triassic Chak Jabbi Limestone is conformable and gradational, while its upper contact is disconformable with the Early Jurassic Datta formation. The Nizampur iron ore deposits have an average grade of 29% iron and 100 million tons of reserves.

3. Methodology

In this study, a comprehensive methodology was employed to investigate the Iron ore mineralization zone in the Nizampur region, Pakistan. Integrating (UAV), ERT surveys, and magnetic survey, and field survey [24] as manifested in Figure 2.

The UAV survey provided surface features of the area, while the magnetic survey identified the magnetic anomaly in the study area. The 2D ERT survey provides detailed, continuous information on iron ore mineralization. This integrated approach aimed to provide a detailed understanding of the geological features and distribution of laterite deposits, essential for effective exploration and resource assessment.

3.1. UAV survey data collection and processing

The DJI Phantom 4 Pro drone was used to capture aerial images of the study area. The UAV system used in this study is shown in Figure 3a. The UAV system specifications, including camera sensor, lens, and battery capacity, are tabulated in Table 1.

The flight path, as shown in Figure 3b, is planned by specifying parameters such as flight routes, altitudes, and image capture boundaries to ensure comprehensive coverage of the area of interest. The UAV was flown at a height of 45 m over the study area, with 80 and 60% frontal and lateral overlaps, respectively.

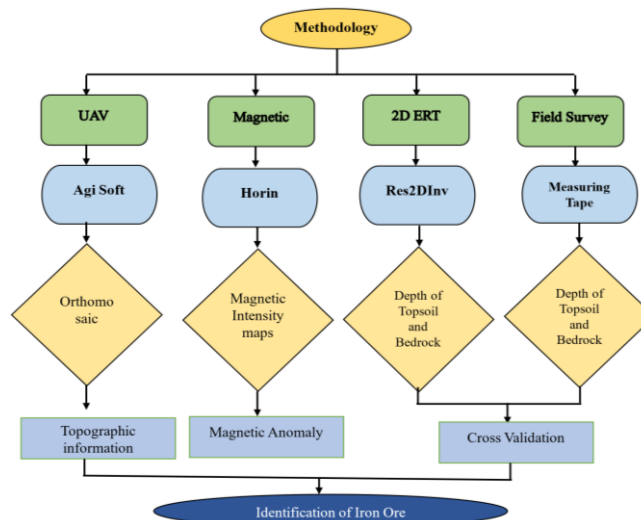


Figure 2. Methodology flow chart

Table 1. Specification of DJI Phantom 4 Pro

UAV model name	DJI Phantom 4 Pro
Weight (battery & propellers included)	1388 g
Max flight time	Approx. 30 minutes
Camera sensor	1'' CMOS Effective pixels: 20M
Camera lens	FOV 84° 8.8 mm/24 mm (35 mm format equivalent) f/2.8 – f/11 auto focus at 1 m – ∞
Photo	JPEG, DNG (RAW), JPEG + DNG
Supported SD cards	Micro SD
Battery	Max Capacity: 128GB
Battery	6000 mAh LiPo 2S
Mobile app/ live view	DJI GO 4
Remote controller max Transmission distance	4 km
UAV model name	DJI Phantom 4 Pro

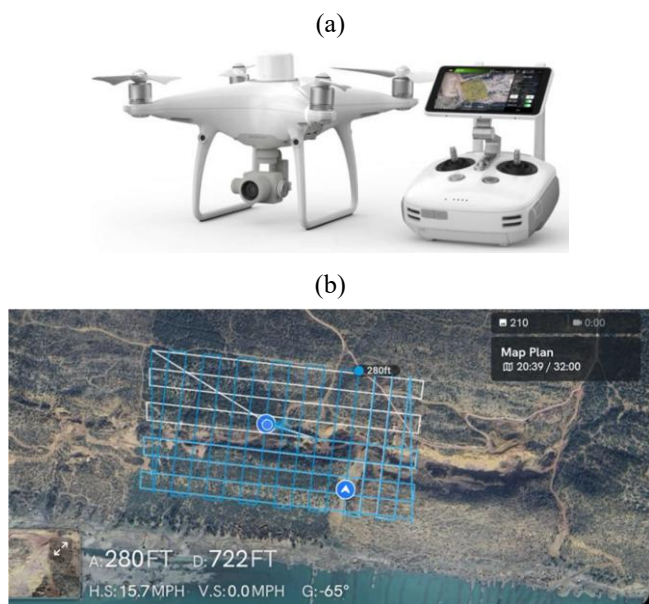


Figure 3. UAV Survey (a) UAV system used (b) flight path

After data collection, the aerial images were imported into Agisoft Metashape to produce a 3D point cloud using the Structure-from-Motion (SfM) algorithm. Once the 3D point cloud was generated, georeferencing was performed using Ground Control Points (GCPs) with known geographic coordinates.

3.2. 2D electrical resistivity (2D ERT) survey

Eight Electrical Resistivity Tomography (ERT) profiles parallel to the iron ore mineralization zone were acquired. The Agi Super Sting R1 IP meter was used for data acquisition, using the Schlumberger protocol, as it provides good vertical resolution [25]. The purpose of the ERT survey was to verify the thickness of the overburden and determine the depth of the iron ore at the site. Each profile was limited to a maximum length of 84 meters, with electrodes spaced at 6-meter intervals. The precise details of each profile, including electrode arrangement and specific survey conditions, are comprehensively documented in Table 2.

Table 2. Description of 2D ERT Survey Line Geometry

Survey line	Direction	Site	No. of electrodes	Electrode spacing, m	Line, length, m
ERT-P1	Northeast	Nizampur laterite ore deposit	14	6	84
ERT-P2	Southeast				
ERT-P3	Northwest				
ERT-P4	North south				
ERT-P5	North South				
ERT-P6	Southwest				
ERT-P7	Southeast				
ERT-P8	East west				
ERT-P1	Northeast				
ERT-P2	Southeast				

The collected ERT data were processed in RES2Dinv to produce a subsurface ERT tomograph. First, the bad data points were removed, followed by forward modelling. After forward modelling, least-squares optimization was performed to obtain the true subsurface resistivities. Several iterations were performed to obtain the low rms value.

3.3. Field survey

The purpose of the field survey was to authenticate the magnetic and 2D ERT interpretation. The thickness of the topsoil and laterite ore was measured using a tape measure in the exposed area. The purpose of the field survey was to validate the outcome of the 2D ERT and magnetic survey. The measuring tape was hung from the top of the exposed face in the area. A person standing opposite the face noted the thickness of the topsoil and laterite ore through the tape. The field survey enables ground-truthing of the estimated depth and thickness of laterite ore obtained from magnetic and ERT surveys.

3.4. Magnetic survey data collection and processing

The magnetic survey in the study area was conducted in two phases using a GPM-10 Proton magnetometer. In the first phase, magnetic data were collected along eight profiles. These eight magnetic profiles aimed to identify the magnetic anomaly and its depth. Furthermore, the purpose of acquiring these eight magnetic profiles was to validate the ERT survey results. Once the magnetic anomaly was identified, magnetic data were collected along additional profiles, arranged in a grid throughout the study area, to estimate the area covered by iron ore mineralization. The magnetic station locations for the gridded data were sparsely distributed, as shown in Figure 4.

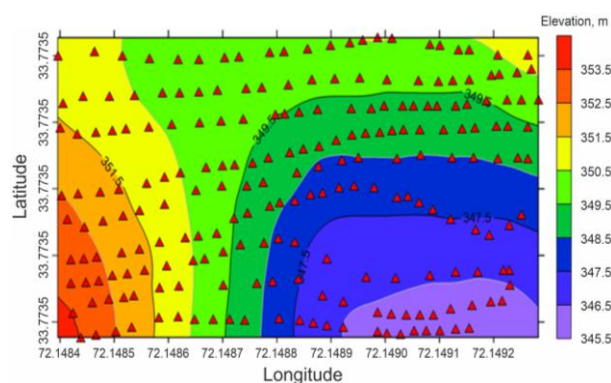


Figure 4. Magnetic survey acquisition stations

Each profile was 80 meters long, with magnetic readings recorded at 6-meter intervals to ensure comprehensive spatial coverage and resolution. To enhance the accuracy and reliability of magnetic data, a local base station was established. This station continuously monitored background magnetic noise and served as a calibration reference, enabling correction of temporal variations in the Earth's magnetic field.

Post-survey, the raw data were systematically converted into CSV format, facilitating easy handling and compatibility with various data processing software. Initially, the diurnal correction was applied by adjusting the collected data for diurnal variations. After the diurnal correction, the data were imported into Horin geophysical software for further processing. The Horin software successfully provided the total magnetic map and its derivatives for the detailed assessment of iron ore mineralization.

4. Results

This section presents the findings from the UAV, ERT, and magnetic survey conducted in the study area. Each method provided valuable insights into the geological characteristics

and mineralization of laterite ore. The UAV survey was utilized to generate a high-resolution Digital Elevation Model (DEM), revealing the topographic variations of the study site. The ERT survey helped identify subsurface layers, including the topsoil, transition zone, and laterite ore, based on resistivity variations. The magnetic survey detected magnetic anomalies associated with iron-rich laterite deposits, and forward modeling was used to estimate their depth and extent. The combination of these geophysical techniques provided a detailed and reliable assessment of laterite mineralization, which was further validated through field measurements.

4.1. UAV survey

The 3D point cloud of the study area was reconstructed from 558 high-resolution aerial images as provided in Figure 5a. The 3D point cloud was further processed to obtain the Digital Elevation Model (DEM) depicted in Figure 5b.

Figure 5b shows that the elevation in the study area ranges from 218 to 342 m. The color gradient, spanning from blue to red, indicates distinct height tiers, with blue denoting lower elevations and red higher elevations. The Digital Elevation Model (DEM), combined with a 3D point cloud, was utilized to plan the profiles for ERT and magnetic data acquisition.

4.2. Electric resistivity tomography

Figure 6 and 7 show the interpretation of eight ERT profiles conducted in the study area. As laterite is a mixture of iron ore and other minerals, the reddish colour indicates it is laterite ore. The resistivity of laterite ore ranges between 700 and 1200 ohm.m. The topmost layer up to 3 m, shown in blue, is characterized as topsoil.

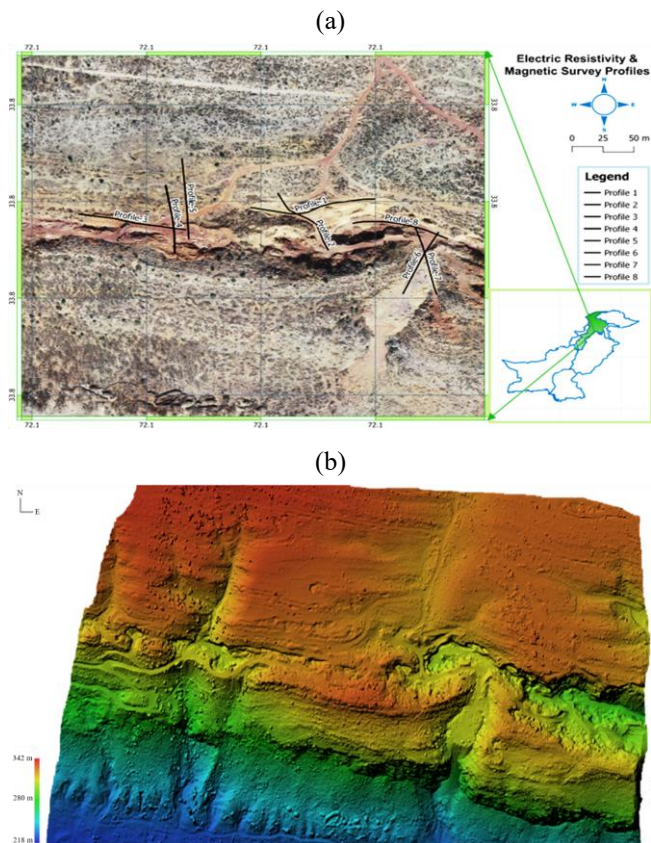


Figure 5. Digital elevation model (DEM) of the study area: (a) 3D point cloud; (b) DEM

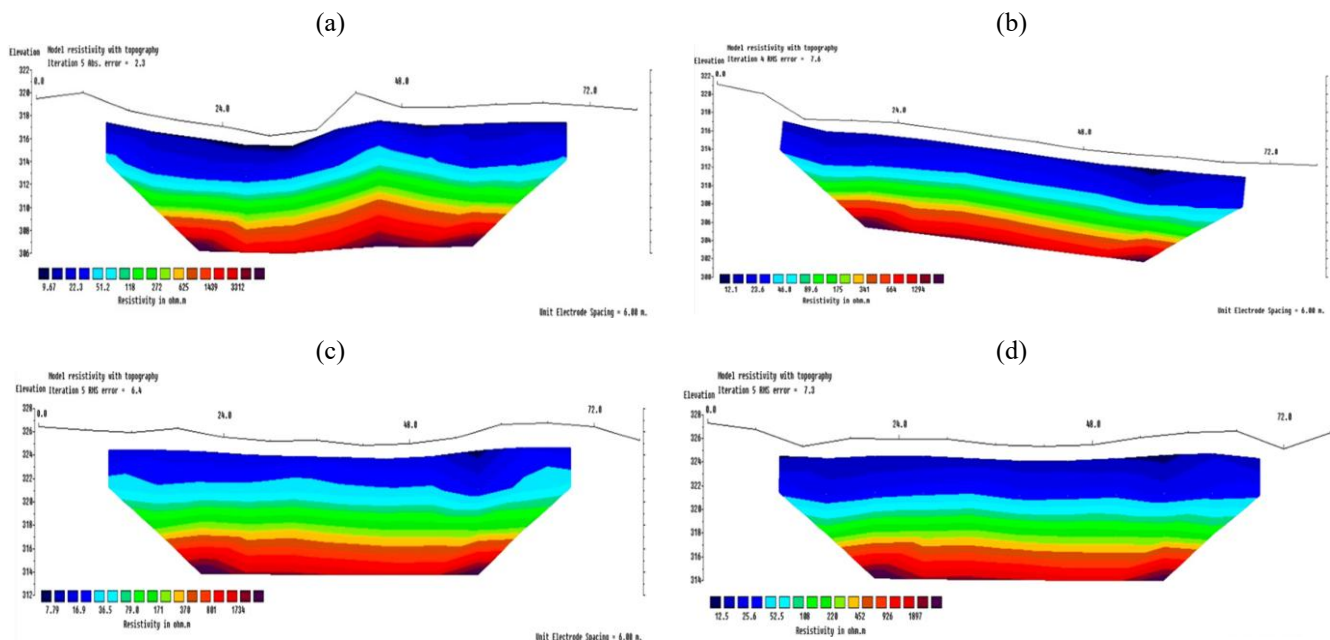


Figure 6. 2D ERT interpretation: (a) profile 1; (b) profile 2; (c) profile 3; (d) profile 4

The resistivity of topsoil ranges from 10 to 50 ohm.m. The resistivity values between 50 and 600 ohms are identified as the transition zone between topsoil and laterite ore. The thickness of this layer was around 3-4 m.

4.3. Field survey

In the exposed area, the thickness of the topsoil and bedrock was also measured with a tape measure. The field

survey indicates that the overburden thickness in the study area was 3 m of topsoil, 2 m of shale, and 2 m of laterite ore, as shown in Figure 8.

The field survey measurements reveal that the laterite ore is at around 5 m depth in the study area and is well supported by magnetic and 2D ERT surveys. Hence, the magnetic data obtained in this study are reliable and can be used to identify laterite ore mineralization zones.

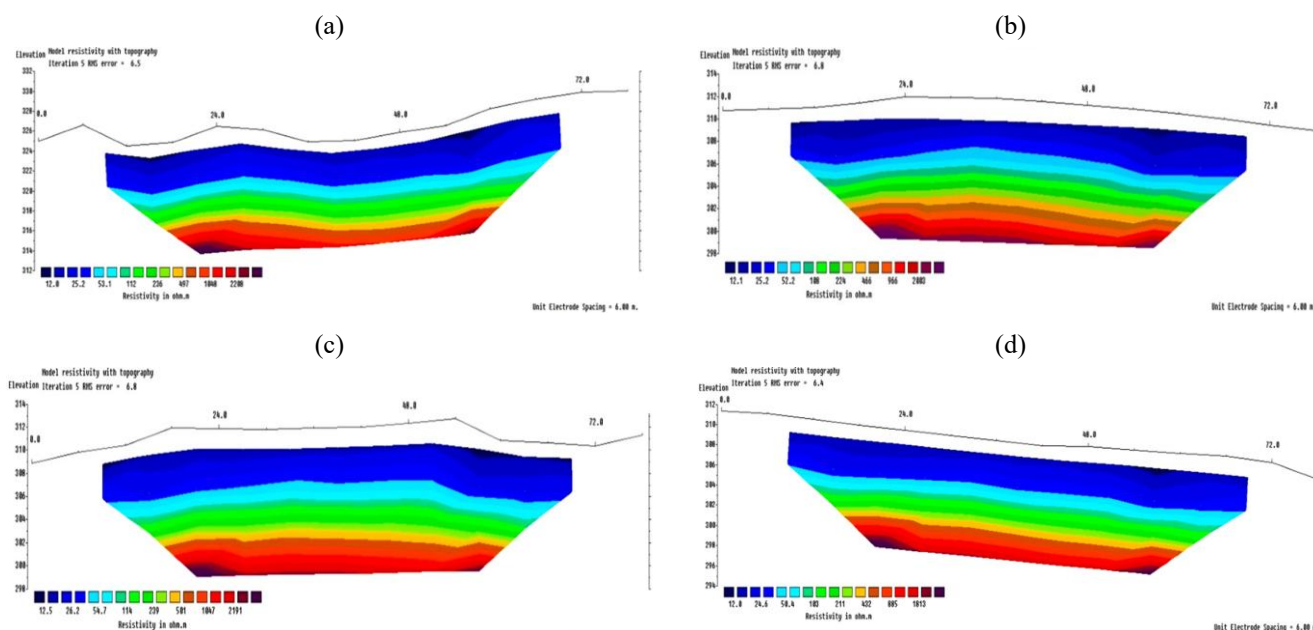


Figure 7. 2D ERT Interpretation: (a) profile 5; (b) profile 6; (c) profile 7; (d) profile 8

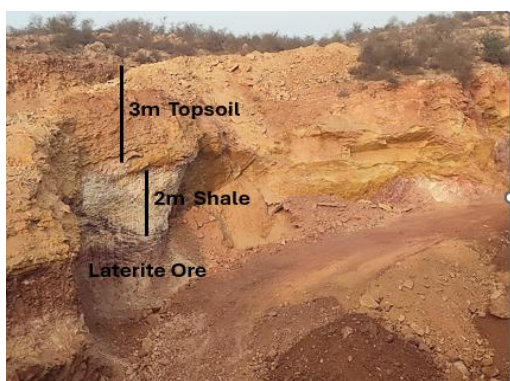


Figure 8. Thickness of Topsoil, Shale and Iron Ore obtained through the Feld Survey

4.4. Magnetic survey

The graphical interpretation of magnetic profiles is shown in Figure 9. The interpretation reveals noticeable variations in magnetic field intensity, indicating the presence of magnetic anomalies in the study area.

The magnetic values recorded by eight profiles vary from 350 to 750 nT. A magnetic anomaly of various intensity was identified in the study area. In magnetic profiles 1-6, a magnetic anomaly of approximately 120 nT was identified. Whereas profiles 7 and 8 show stronger magnetic anomalies of around 250 and 200 nT, respectively. In contrast, profile 8 reveals a magnetic anomaly of 100 nT. Therefore, to identify the hypothetical depth of this magnetic anomaly, forward modelling was performed, as shown in Figure 10.

Figure 10 reveals that the depth of the magnetic anomaly in profiles 1, 2, 3, 4, 5, and 8 is around 5 m. Whereas the magnetic anomalies at profiles 6 and 7 have higher magnetic intensity and are located at about 3 m depth.

Once the reliability of the magnetic survey is confirmed and validated with 2D ERT and field survey, a total magnetic intensity maps were established from gridded data. The gridded data from these stations were used to produce a detailed total magnetic anomaly (TMA) map of the study area using Horin geophysical software, as depicted in Figure 11a.

The TMA map was established by subtracting the inter-nation geomagnetic reference field (IGRF) from the recorded data as described in Figure 11a. The noise in the form of a spark was removed from the data. The TMA map identified a strong magnetic anomaly towards the north-western part, while lower towards the south-eastern direction. The strong magnetic anomaly is represented by the brown and pink colors, with a total magnetic intensity exceeding 650 nT. These anomaly patterns suggest lithological variations, with the highs potentially representing magnetite-rich or intrusive bodies, whereas the lows indicate demagnetized or weakly magnetic lithologies.

In the next phase, the north magnetic pole was selected as the reduction point for the gridded TMA map to establish the reduced-to-pole RTP map. To compensate for the distortion caused by the Earth's magnetic field, 530 inclinations and 30 degrees for declination were used. The RTP map (Fig. 11b) also confirmed a magnetic anomaly of around 200-300 nT in the south-west direction.

The upward continuation map at 100 m also clearly reveals the regional distribution of magnetic anomalies within the study area, as depicted in Figure 11c. A broad, strong magnetic intensity anomaly is observed in the western part of the study area, indicated by pink to red colors. Its persistence after upward continuation indicates that a deep, strongly magnetized body is responsible. This feature is interpreted as a major magnetic high that likely marks a significant structural block within the basement. In contrast, towards the central and southeastern portions of the study area, moderate to low magnetic responses represented by green to blue were observed.

5. Discussion

The accurate delineation of iron ore mineralization zones within lateritic deposits is crucial for efficient mine planning and development. Reliable estimation of the iron ore mineralization zone depends on accurate topographic information, precise estimation of topsoil thickness, and accurate characterization of the ore body.

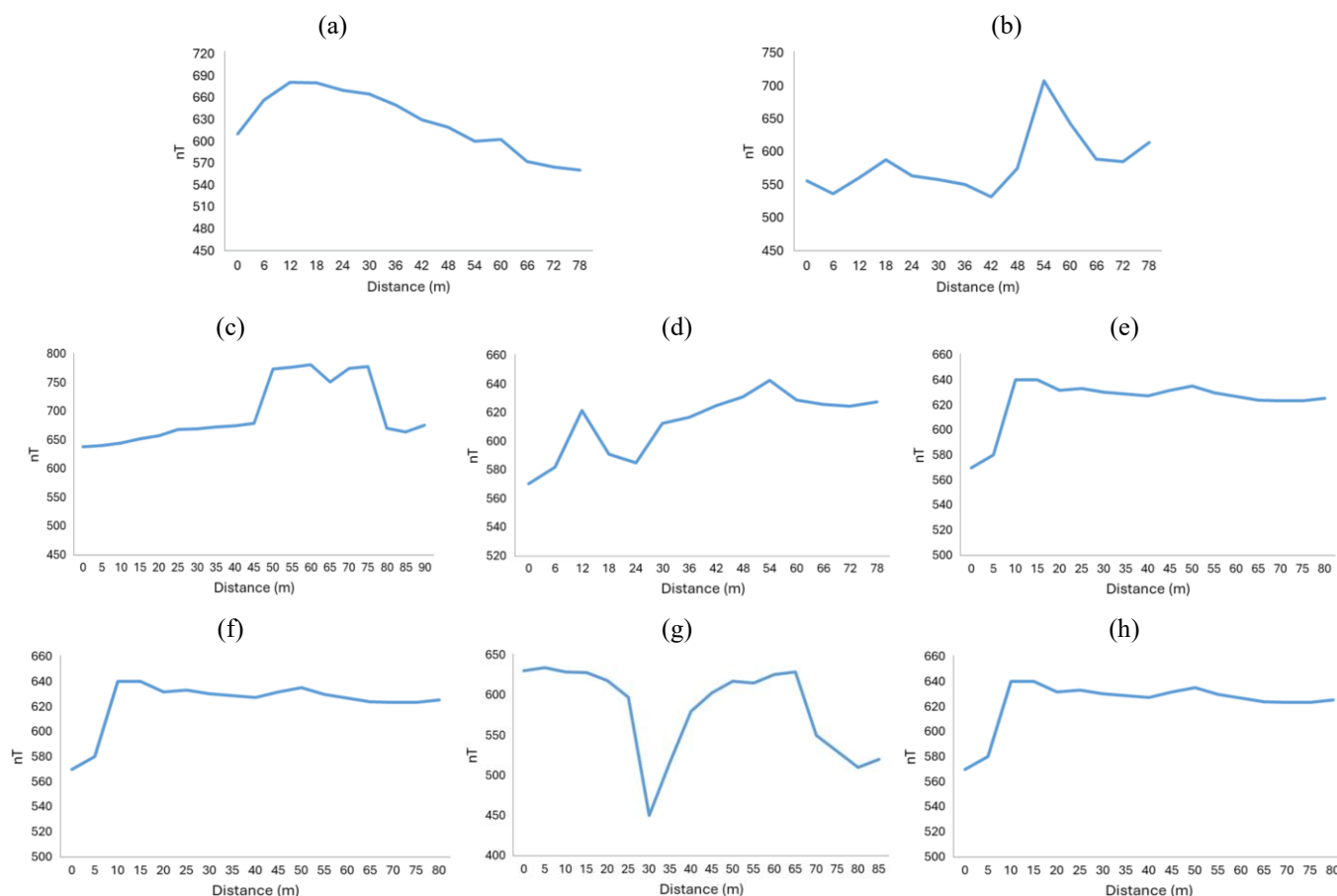


Figure 9. Magnetic data interpretation: (a) profile 1; (b) profile 2; (c) profile 3; (d) profile 4; (e) profile 5; (f) profile 6; (g) profile 7; (h) profile 8

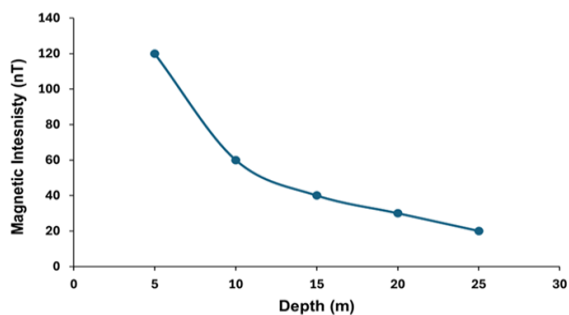


Figure 10. Magnetic intensity vs depth

For this purpose, an integrated approach is required. Considering the low commodity price of laterite ore, the adopted approach should be cost-effective. In this study, an effective approach was applied by integrating UAV, magnetic and ERT for detailed characterization of iron ore mineralization.

The UAV survey successfully captured high-resolution aerial images of the study area, enabling the reconstruction of high-resolution digital elevation models. This enables the extraction of detailed topographic information required for planning ERT and magnetic profiles [26]. The orthomosaic generated from UAV imagery indicates that the elevation within the study area ranges from 218 to 342 m.

To obtain the precise depth of topsoil and laterite ore, ERT is the most reliable method. Falade et al. [27] adopted a similar methodology. An analysis of the resistivity profiles reveals stratified deposits within the surveyed area. At the surface, the top-soil layer exhibits resistivity values ranging from 10 to 50 ohms.m, indicative of its composition and

moisture content, as concluded by Koah Na Lebogo, Zame [28]. Beneath the topsoil lies a shale layer with resistivity ranging from 50 to 150 ohm.m, suggesting a distinct lithological change. Further down, the resistivity values increase significantly to a range of 150-1200 ohm.m, indicating the presence of a laterite ore layer. The thickness of these layers is delineated with precision: the topsoil extends to a depth of 3 meters, followed by a 2-meter-thick shale layer, and the laterite ore body begins at a depth of 5 meters below the ground surface. The field measurements at the exposed area validated the estimates of the thickness of the topsoil and the iron ore bedrock.

The magnetic survey successfully identified a magnetic anomaly of approximately 200 nT in the study area. Forward modelling was performed to estimate the depth of the magnetic anomaly, as indicated by Zhao et al. [29]. Forward modelling allows for the estimation of the depth of the magnetic anomaly at each profile. Based on forward modelling, the magnetic anomalies along profiles 1, 2, 3, 4, 5, and 8 occur at a depth of around 5 m, while the anomaly along profiles 6, 7, and 7 occurs at a depth of 3 m. To understand the detailed pattern of the magnetic anomaly in the study area, the total magnetic intensity (TMI) map was produced. The TMI map reveals the lithological variations within the study area. The high magnetic anomaly of more than 600 nT potentially represents magnetite-rich or intrusive bodies [30], whereas the lows indicate demagnetized or weakly magnetic lithologies. Numerous linear gradients in the TMI map are aligned NW-SE and NE-SW, which may reflect major structural discontinuities or faults [31].

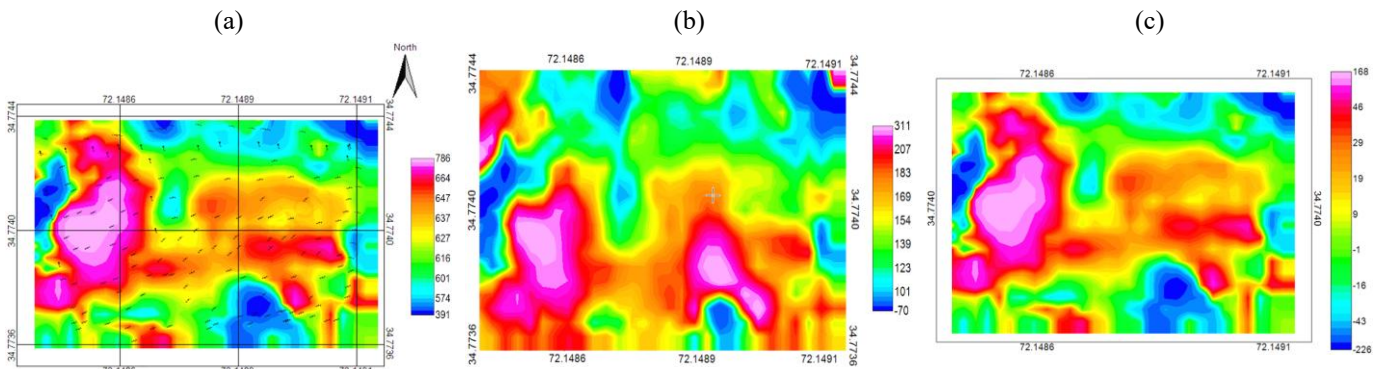


Figure 11. Magnetic maps: (a) total magnetic intensity; (b) reduced to pole; (c) continuation

The removal of dipolar effects by producing the RTP map enhances the symmetry of anomalies, enabling a more direct correlation between magnetic highs/lows and their source lithologies [32]. In addition, the continuation map suppresses near-surface anomalies and emphasizes longer-wavelength signals, allowing for clearer recognition of deep-seated structures. The continuation map shows that the high magnetic-intensity anomaly occurs in the western part of the area, where it is associated with a deep, strongly magnetized body. On the other hand, the central and southeastern portions of the study area exhibit moderate to low magnetic responses. Furthermore, gradual east-west transitions from magnetic highs to lows suggest the presence of regional fault systems or lithological boundaries at depth.

Cross-validation of magnetic survey results with ERT and field measurements indicates that magnetic surveys can identify the iron-ore mineralization zone in a lateritic deposit. The integrated approach adopted in this study enables the successful delineation of the iron ore mineralization zone and provides precise thicknesses for the topsoil and iron ore body. Thus, the integrated UAV, ERT and magnetic approach adopted in this study is thus mooted as rapid, expeditious and reliable compared to the conventional drilling technique.

6. Conclusions

This research demonstrates the effectiveness of integrating UAV, magnetic, and ERT surveys to delineate laterite ore deposits in the Nizampur region of Khyber Pakhtunkhwa, Pakistan. The UAV survey provides a precise topographic map and an orthomosaic of the study area, which were essential for planning geophysical profiles and understanding surface morphology. The elevation difference based on the UAV survey ranged from 218 to 342 m. The acquired eight ERT profiles identified three geological layers in the study area. The reliable depths of the topsoil, shale, and laterite ore were estimated at 3, 2 and 5 m, respectively. The resistivity of the topsoil was characterized as 10-50 ohm.m, shale was identified by 50-700 ohm.m, whereas the laterite ore was identified by 150 to 1200 ohm.m.

Magnetic survey results, supported by forward modeling, identified shallow magnetic anomalies associated with iron ore mineralization, with magnetic intensities of around 650 nT. The forward modelling successfully estimated the depth of the magnetic anomaly. In contrast, the TMI, RTP and continuation maps reveal the distribution of magnetic anomaly in the study area. Based on these methods, it is concluded that the northwestern part of the deposit has a rich distribution of iron ore. In addition, the RTP and con-

tinuation maps reveal possible structural discontinuities in the study area. The findings of this research work are concluded as follows.

1. UAV surveys provided reliable and high-resolution DEM and orthomosaics, enabling detailed topographic mapping and optimized planning of geophysical profiles.

2. ERT results in reliably characterized subsurface stratigraphy, delineating topsoil, shale, and laterite ore layers with precise depth estimates validated by field measurements.

3. Magnetic surveys successfully identified shallow anomalies associated with iron ore mineralization and provided a detailed spreading of the magnetic anomaly in the study area. In addition, the magnetic data in the form of RTP and continuation maps comprehensively revealed structural discontinuities and distinguished between strongly magnetized and weakly magnetic lithologies.

The integration of UAV, ERT, and magnetic methods proved to be a rapid, reliable, and cost-effective alternative to conventional drilling for delineating iron ore mineralization in lateritic deposits.

Author contributions

Conceptualization: MJ, MZE; Data curation: MJ, FK; Formal analysis: MJ, FK, SUS; Funding acquisition: NA; Investigation: MJ, BA, MZE; Methodology: MJ, BA, MZE, TF; Project administration: BA, MZE, TF; Resources: MZE, TF; Software: MJ, BA; Supervision: BA, MZE; Validation: MJ, FK, SUS; Visualization: MJ, SUS, TK; Writing – original draft: MJ, FK, BA, SUS; Writing – review & editing: MZE, TF. All authors have read and agreed to the published version of the manuscript.

Funding

This research received no external funding.

Acknowledgements

Special thanks to Prince Sultan University Riyadh, Saudi Arabia for partly funding this research. The authors also extend special thanks to the Department of Geotechnics and Transportation, National University of Sciences and Technology, Pakistan, for providing the electrical resistivity instruments. We also expressed special thanks to Horin for providing a complimentary educational license for Horin Geophysical software.

Conflicts of interests

The authors declare no conflict of interest.

Data availability statement

The original contributions presented in the study are included in the article, further inquiries can be directed to the corresponding author.

References

- [1] Khan, M.A., Kerr, A.C., Abdullah, Kakar, H.U., Tariq, M., & Naeem, A. (2025). Major and trace elements geochemistry of Ziarat laterite deposits, Ziarat District, western Pakistan. Implications for source rock materials and ore genesis. *Carbonates and Evaporites*, 40(1), 24. <https://doi.org/10.1007/s13146-025-01063-7>
- [2] Elias, M. (2002). Nickel laterite deposits-geological overview, resources and exploitation. *Giant Ore Deposits: Characteristics, Genesis and Exploration. CODES Special Publication*, 4, 205-220.
- [3] Freyssinet, P.H., Butt, C.R.M., Morris, R.C., & Piantone, P. (2005). Ore-forming processes related to lateritic weathering. *One Hundredth Anniversary Volume*. <https://doi.org/10.5382/av100.21>
- [4] Traoré, D.L., Traoré, S., & Diakitè, S. (2014). Bauxite industry in guinea and value opportunities of the resulting red mud as residue for chemical and civil engineering purposes. *Journal of Civil Engineering Research*, 4(1), 14-24.
- [5] Marut, J.J., Alaezi, J.O., & Igwe, C.O. (2020). A review of alternative building materials for sustainable construction towards sustainable development. *Journal of Modern Materials*, 7(1), 68-78. <https://doi.org/10.21467/jmm.7.1.68-78>
- [6] Anger, B., Moulin, I., Commene, J.P., They, F., & Levacher, D. (2019). Fine-grained reservoir sediments: An interesting alternative raw material for Portland cement clinker production. *European Journal of Environmental and Civil Engineering*, 23(8), 957-970. <https://doi.org/10.1080/19648189.2017.1327890>
- [7] Chen, L., Wang, H., Sun, C., Chang, X., & Ding, W. (2025). The application of integrated geochemical and geophysical exploration for prospecting potential prediction of copper and gold polymetallic deposits in the Fudiyngzi-Bacheli Area, Heilongjiang Province. *Minerals*, 15(6), 597. <https://doi.org/10.3390/min15060597>
- [8] Okada, K. (2022). Breakthrough technologies for mineral exploration. *Mineral Economics*, 35(3), 429-454. <https://doi.org/10.1007/s13563-022-00317-3>
- [9] Aleva, G.J.J. (1994). *Laterites: Concepts, geology, morphology and chemistry*. Wageningen, Netherlands: International Soil Reference and Information Center, 169 p.
- [10] Dahlin, T. (1996). 2D resistivity surveying for environmental and engineering applications. *First Break*, 14(7). <https://doi.org/10.3997/1365-2397.1996014>
- [11] La Salandra, M., Nicotri, S., Donvito, G., Italiano, A., Colacicco, R., Miniello, G., & Capolongo, D. (2024). A paradigm shift in processing large UAV image datasets for emergency management of natural hazards. *International Journal of Applied Earth Observation and Geoinformation*, 132, 103996. <https://doi.org/10.1016/j.jag.2024.103996>
- [12] Junaid, M., Abdullah, R.A., Abdelrahman, K., Ullah, A., Mahmood, S., Sa'ari, R., & Islam, A. (2024). Assigning resistivity values to rock quality designation indices using integrated unmanned aerial vehicle and 2D electrical resistivity tomography in granitic rock. *Geocarto International*, 39(1), 2343019. <https://doi.org/10.1080/10106049.2024.2343019>
- [13] Assali, P., Grussenmeyer, P., Villemin, T., Pollet, N., & Viguier, F. (2014). Surveying and modeling of rock discontinuities by terrestrial laser scanning and photogrammetry: Semi-automatic approaches for linear outcrop inspection. *Journal of Structural Geology*, 66, 102-114. <https://doi.org/10.1016/j.jsg.2014.05.014>
- [14] Dentith, M., & Mudge, S.T. (2014). *Geophysics for the mineral exploration geoscientist*. Cambridge, United Kingdom: Cambridge University Press, 438 p. <https://doi.org/10.1017/CBO9781139024358>
- [15] Malkani, M.S., & Mahmood, Z. (2016). Mineral resources of Pakistan: A review. *Geological Survey of Pakistan, Record*, 128, 1-90.
- [16] Jaffar, A., Ali, N., Anwer, M., Naeem, M.A., Riaz, M.R., Jamal, M.H., & Ming, X. (2014). The impact of cement manufacturing on economic development of Pakistan: The analysis of cement industry. *International Journal of Research*, 2, 205-220.
- [17] Malkani, M.S., Khosa, M.H., Alyani, M.I., Khan, K., Somro, N., Zafar, T., & Zahid, M.A. (2017). Mineral deposits of Khyber Pakhtunkhwa and FATA, Pakistan. *Lasbela University Journal of Science and Technology*, 6, 23-46.
- [18] Abdullah, R.A., Junaid, M., Sa'ari, R., Ali, W., Islam, A., & Sari, M. (2022). 3D modelling and feasibility assessment of granite deposit using 2D electrical resistivity tomography, borehole, and unmanned aerial vehicle survey. *Journal of Mining and Environment*, 13(4), 929-942. <https://doi.org/10.22044/jme.2022.11938.2189>
- [19] Junaid, M., Abdullah, R.A., Sa'ari, R., Ali, W., Rehman, H., Alel, M.N.A., & Ghani, U. (2021). 2D electrical resistivity tomography an advance and expeditious exploration technique for current challenges to mineral industry. *Journal of Himalayan Earth Sciences*, 54(1), 11-32.
- [20] Sehad, S., & Raharjo, S.A. (2017). Application of magnetic survey to explore the iron ore deposits in the Nusawungu coastal regency of Cilacap Central Java. *Jurnal Penelitian Fisika Dan Aplikasinya (JPFA)*, 7(2), 79-88. <https://doi.org/10.26740/jpfa.v7n2.p79-88>
- [21] Malkani, M.S., Mahmood, Z., Alyani, M.I., & Shaikh, S.I. (2017). Revised stratigraphy and mineral resources of Sulaiman Basin, Pakistan. *Geological Survey of Pakistan, Information Release (GSP IR)*, 1003, 1-63.
- [22] Siddiqui, C.M.R.H., Haidar, N., & Hussain, A. (2024). Mineralogy and genesis of Nizampur iron ore, KPK, Pakistan. *Geologica: An International Journal of Earth Sciences*, 7(1), 3-21.
- [23] Nasir, M.J., Tufail, M., Ayaz, T., Khan, S., Khan, A.Z., & Lei, M. (2022). Groundwater quality assessment and its vulnerability to pollution: A study of district Nowshera, Khyber Pakhtunkhwa, Pakistan. *Environmental Monitoring and Assessment*, 194(10), 692. <https://doi.org/10.1007/s10661-022-10399-9>
- [24] Sapia, V., Villani, F., Improta, L., Fischanger, F., De Martini, P.M., Romano, V., & Lupi, M. (2025). Combining 3-D deep electrical resistivity tomography with magnetic surveys to investigate complex tectonic basins: A case study from the central Apennines seismic belt (Italy). *Tectonics*, 44(9), e2024TC008716. <https://doi.org/10.1029/2024TC008716>
- [25] Khalil, M.A., & Santos, F.A.M. (2013). 2D and 3D resistivity inversion of Schlumberger vertical electrical soundings in Wadi El Natrun, Egypt: A case study. *Journal of Applied Geophysics*, 89, 116-124. <https://doi.org/10.1016/j.jappgeo.2012.11.014>
- [26] Busato, L., Boaga, J., Peruzzo, L., Himi, M., Cola, S., Bersan, S., & Cassiani, G. (2016). Combined geophysical surveys for the characterization of a reconstructed river embankment. *Engineering Geology*, 211, 74-84. <https://doi.org/10.1016/j.enggeo.2016.06.023>
- [27] Falade, A.O., Bewaji, S., & Olagunju, B.D. (2025). Electrical resistivity and magnetotelluric integration for groundwater exploration at the proposed central library in Achievers University Owo, Nigeria. *Discover Geoscience*, 3(1), 99. <https://doi.org/10.1007/s44288-025-00212-8>
- [28] Koah Na Lebogo, S.P., Zame, P.Z.O., Anaba Onana, A.B., Kamenji, F.S., Gwet, H., & Bisso, D. (2025). Assessment of groundwater rise zones using electrical resistivity for foundation stability analysis. *Discover Geoscience*, 3(1), 109. <https://doi.org/10.1007/s44288-025-00216-4>
- [29] Zhao, P., Wu, Z., Han, X., Wang, Y., Zhang, J., & Wang, Q. (2025). The structure and near-bottom magnetic anomaly characteristics of the Daxi Vent Field on the Carlsberg Ridge, Northwestern Indian Ocean. *Journal of Marine Science and Engineering*, 13(3), 488. <https://doi.org/10.3390/jmse13030488>
- [30] Liu, Y.X., Li, W.Y., Liu, Z.Y., Zhao, J.W., Cao, A.Q., Gao, S., & Yang, C. (2022). Occurrence characteristics of magnetite and aeromagnetic prospecting northeast of Hebei Province. *Minerals*, 12(9), 1158. <https://doi.org/10.3390/min12091158>
- [31] Eshanibli, A., Ismail, N.A., Ghanush, H.B., Dugdug, A., Uyimwen, O.A., Khalifa, N., & Khalf, K.A. (2025). Delineation of depth to basement and subsurface structures beneath the Gerad Graben, western Sirt Basin, Libya, from gravity and aeromagnetic data. *Energy Geoscience*, 6(4), 100468. <https://doi.org/10.1016/j.engeos.2025.100468>
- [32] Wemegah, D.D., Preko, K., Noye, R.M., Boadi, B., Menyeh, A., Danuor, S.K., & Amenyoh, T. (2015). Geophysical interpretation of possible gold mineralization zones in Kyerano, South-Western Ghana using aeromagnetic and radiometric datasets. *Journal of Geoscience and Environment Protection*, 3(4), 67-82. <https://doi.org/10.4236/gep.2015.34008>

Інтегрований геофізичний підхід і аерофотограмметрія для детального оконтурювання залізородної мінералізації в латеритних відкладах

М. Джунайід, Ф. Хан, Б. Альшамері, С.У. Шах, М.З. Емад, Т. Ферозе

Мета. Дослідження інтеграції безпілотних літальних апаратів (БПЛА), магнітної зйомки та двовимірної електророзвідувальної томографії (2D ERT) для оконтурювання зон латеритної рудної мінералізації у приповерхневому просторі зі зниженням витрат на геологорозвідувальні роботи.

Методика. У дослідженні застосовано комплекс UAV-зйомки, магнітної зйомки, двовимірної електророзвідувальної томографії та польової верифікації. UAV-зйомку використано для фіксації поверхневих особливостей ділянки та планування профілів. Магнітні вимірювання за профільною і сітковою схемами з діурнальною корекцією дали змогу виявити аномалії та оконтурити зону мінералізації. ERT застосовано для деталізації літологічної будови, виділення ґрунтового покриву, сланців і латеритових утворень, а також уточнення глибини й потужності рудного шару. Польові вимірювання використано для перевірки геофізичних результатів.

Результати. За даними ERT встановлено, що потужність верхнього ґрунтового шару становить 3 м, а його питомий електричний опір змінюється в межах 10-50 Ом·м. Для шару сланців отримано значення питомого опору 50-150 Ом·м за потужності близько 2 м. Ідентифіковано латеритну руду за значеннями питомого електричного опору в діапазоні 150-1200 Ом·м і потужністю до 5 м. За результатами магнітної зйомки виявлено аномалії інтенсивністю 200-600 нТл, глибина залягання яких за даними прямого моделювання оцінена в межах 3-5 м. Інтерпретація на регіональному рівні за картами повної напруженості магнітного поля (ТМІ), трансформації з приведенням до полюса (RTP) та картами продовження дала змогу деталізувати просторовий розподіл магнітних аномалій у межах досліджуваної території, встановити літологічні неоднорідності, елементи розривної тектоніки та глибокозалягаючі магнітно активні тіла.

Наукова новизна. Запропоновано інтегрований маловитратний підхід до виявлення латеритної мінералізації, який поєднує детальні геофізичні дослідження, зокрема магнітні методи, 2D ERT та фотограмметрію з БпЛА. На відміну від традиційних підходів, така схема є економічно доцільнішою з огляду на вартість рудного об'єкта.

Практична значимість. Отримані результати підтверджують, що поєднання аерофотограмметрії, магнітної зйомки та двовимірної електророзвідувальної томографії є ефективним і економічно обґрунтованим підходом до оконтурювання зон латеритної залізорудної мінералізації та може розглядатися як дієва альтернатива традиційним методам геологорозвідки.

Ключові слова: латеритна руда; електророзвідувальна томографія; магнітна зйомка; безпілотний літальний апарат; розвідка корисних копалин

Publisher's note

All claims expressed in this manuscript are solely those of the authors and do not necessarily represent those of their affiliated organizations, or those of the publisher, the editors and the reviewers.